Section 6

Developments in global forecast models, case studies, predictability investigations, global ensemble, monthly and seasonal forecasting

Seasonal re-forecasts of the winter NAO with EC-Earth

L. Batté[(1)], J. García-Serrano[(2)], V. Guemas[(1,3)], M. Asif[(3)], I. Andreu-Burillo[(3,4)] and F.J. Doblas-Reyes[(3,5)]

[1]CNRM-GAME, Météo-France, Toulouse, France (lauriane.batte@meteo.fr) - [2]LOCEAN/IPSL, Université Pierre et Marie Curie, Paris, France - [3]IC3, Barcelona, Spain - [4]Independent scholar - [5]ICREA, Barcelona, Spain

The North Atlantic Oscillation (NAO) is the main mode of variability of the North Atlantic large-scale atmospheric circulation at monthly to interannual time scales. The relationship between the NAO and storm tracks, temperature and precipitation conditions over the North Atlantic basin and adjacent regions justifies the interest in evaluating the seasonal forecast quality of its state (i.e. the value of the NAO index), especially in winter. Previous studies (e.g. Doblas-Reyes et al., 2003; Palmer et al., 2004; Arribas et al., 2011; Kim et al., 2012) have highlighted the limited seasonal forecast skill of global coupled models in predicting the NAO index. Recent seasonal prediction experiments with the EC-Earth Earth system model (Hazeleger et al., 2012; Du et al., 2012) provide interesting perspectives for improving the winter NAO forecast skill.

A first set of experiments consisted in increasing ocean and atmosphere resolution in the EC-Earth3 ESM. The standard resolution (SR) experiment uses a T255L91 grid for the atmosphere (IFS) and ORCA1 grid with 46 vertical levels for the ocean (NEMO-LIM). The high resolution configuration (HR) implies increasing the IFS horizontal resolution to T511 (approximately 40 km) and the NEMO resolution to ORCA025 and 75 vertical levels. Five-member ensemble forecasts were run starting from ERA-Interim (Dee et al., 2011) and GLORYS2v1 (Ferry et al., 2010) reanalyses every November over 1993-2009 up to four forecast months.

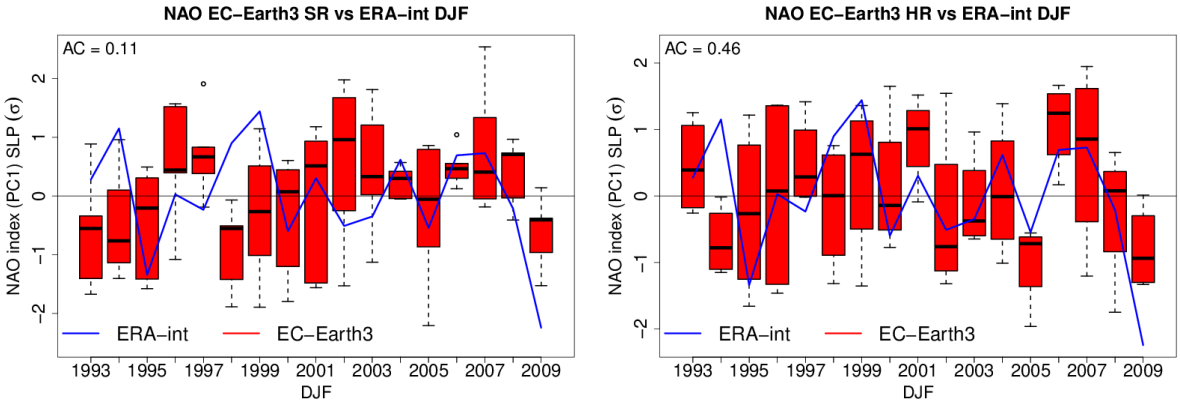

Fig. 1: DJF NAO index in the EC-Earth3 SR (left) and HR (right) hindcasts (red boxes and whiskers) using the Pobs method (see Doblas-Reyes et al. 2003); the black line is the ensemble median and the anomaly correlation between the ensemble mean index and ERA-Interim reanalysis (in blue) is given in the top left corner. Note that undetrended sea-level pressure anomalies have been considered. The year in the abscissa corresponds to that of the start date (first of November of each year).

Results for the December-January-February (DJF) NAO are shown in Figure 1. The ERA-Interim NAO index is computed as the leading principal component of sea-level pressure over the North Atlantic region. The anomaly correlation of the model ensemble mean index is higher in HR. The analysis of individual forecasts such as the 2009/10 extreme winter might require a larger ensemble size, which is currently being prepared. Intermediate experiments using high resolution in one of the two main components of EC-Earth3 should shed further light on the sources of improvement.

A second set of experiments was performed with EC-Earth2.3 over the same hindcast period to investigate the role of sea ice initialization. The reference experiment (INIT) was initialized from the ERA-interim and ORAS4 (Mogensen et al., 2011) reanalyses and from the HistEraNudg sea ice reconstruction (Guemas et al., 2014). The sensitivity experiment (CLIM) only differs from INIT in the initialization of the sea ice component from a climatology of HistEraNudg over the 1981-2010 period.

Figure 2 shows the results from this second set of experiments. It is found that there is a substantial increase of the NAO skill in the INIT re-forecasts. This finding suggests that the sea ice cover state, presumably taken into account in INIT, represents a predictability source of the winter Euro-Atlantic atmospheric circulation. The variance explained by the winter NAO is increased in INIT (50.5%) when compared to CLIM (41.5%), getting closer to the observed one (55.0%) but still underestimated. The results also suggest a role played by sea ice initialization in re-forecasting the negative NAO phase of 2009-10.

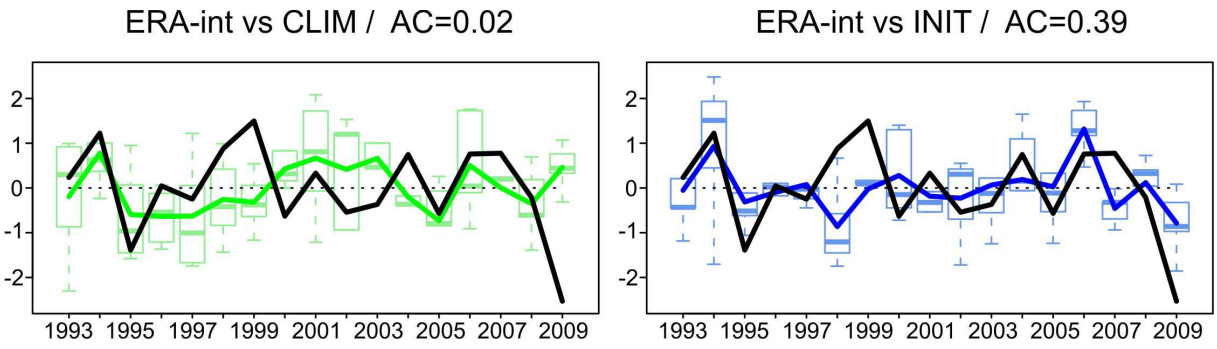

Fig. 2: Same as Fig. 1, but for the seasonal prediction experiments performed with EC-Earth2.3 initialized from climatological sea ice conditions (CLIM; left-green) and realistic sea ice conditions (INIT; right-blue). The ensemble mean index is drawn as a solid line; the anomaly correlation (AC) between the ensemble mean index and ERA-Interim reanalysis (in black) is indicated in the title.

A set of re-forecasts with EC-Earth2.3 where the sea ice restarts will not come from a climatology but from a historical simulation, to have a sea ice state which is approximately in equilibrium with the mean climate at the time of initialization, should allow refining the impact of initializing sea ice variability on the atmosphere skill. Both studies should be extended using longer re-forecast periods and larger ensembles to help draw more robust conclusions.

References:

- Arribas, A. et al. (2011): The GloSea4 ensemble prediction system for seasonal forecasting. Mon. Weath. Rev., 139, 1891-1910.
- Dee, D. P. et al. (2011). The ERA-Interim reanalysis: configuration and performance of the data assimilation system. Q. J. R. Meteorol. Soc., 137, 553–597.
- Doblas-Reyes, F. J., V. Pavan and D.B. Stephenson (2003). The skill of multi-model seasonal forecasts of the wintertime North Atlantic Oscillation. Clim. Dyn., 21: 501-514.
- Du, H. et al. (2012). Sensitivity of decadal predictions to the initial atmospheric and oceanic perturbations. Clim. Dyn., 39, 2013-2023.
- Ferry, N. et al. (2010). Mercator Global Eddy Permitting Ocean Reanalysis GLORYS1V1: Description and Results. Mercator Ocean Quarterly Newsl., 36, 15-27.
- Guemas, V. et al. (2014). Ensemble of sea ice initial conditions for interannual climate predictions. Clim. Dyn., doi: 10.1007/s00382-014-2095-7.
- Hazeleger, W. et al. (2012). EC-Earth V2.2: description and validation of a new seamless earth system prediction model. Clim. Dyn., 39(11): 2611–2629.
- Kim, H.-M., P. J. Webster, and J. A. Curry (2012): Seasonal prediction skill of ECMWF System 4 and NCEP CFSv2 retrospective forecast for the Northern Hemisphere winter. Clim. Dyn., 39, 2957-2973.
- Mogensen, K. S., M. A. Balmaseda and A. T. Weaver (2011). The NEMOVAR ocean data assimilation as implemented in the ECMWF ocean analysis for System 4. ECMWF Technical Memorandum 657.
- Palmer, T.N. et al. (2004). Development of a European multi-model ensemble system for seasonal to inter-annual prediction (DEMETER). Bull. Am. Meteorol. Soc., 85, 853-872.

Acknowledgements: Simulations were run thanks to PRACE HiResClim project and RES national resources at BSC (Spain), and analyses achieved in the framework of the European Commission FP7-SPECS project (grant agreement 308378) and the MINECO-funded PICA-ICE project (CGL2012-31987). J. G.-S. was supported by the FP7-funded NACLIM project (grant agreement 308299).

High resolution and seasonal forecast scores with CNRM-CM5

Michel Déqué[1], Jean-Philippe Piedelievre[1] and Eric Maisonnave[2]
[1]Centre National de Recherches Météorologiques (CNRS/GAME), Météo-France.
42 avenue Coriolis F-31057 Toulouse Cédex 1, France, michel.deque@meteo.fr
[2]Centre Européen de Recherche et Formation Avancée en Calcul Scientifique (CNRS/SUC)
42 avenue Coriolis F-31057 Toulouse Cédex 1, France

Atmospheric and oceanic horizontal resolutions are a key parameter for the realism of the representation of the natural complex system by a set of equations, because the horizontal derivatives are calculated with a better accuracy, and because important forcings like orography, bathymetry or land/sea distribution involve scales from 1000 to less than 1 km. In short-range prediction, high resolution is essential, because the initial state of the system is observed at high resolution, and because time and space accuracy is required for the forecasts. From the 1970s to today, increases in resolution have been quasi-systematically followed by increases in forecast quality. In seasonal prediction, the target concerns continental scales. In addition, past experience has shown that a good representation of physical processes and large ensembles were essential for seasonal skill: the computation cost implied thus restrictions on horizontal resolution. In this study we explore the role of horizontal resolution in both the atmosphere and the ocean on the predictability of two major phenomena at seasonal scale: ENSO and NAO.

We used here the CNRM-CM5 model (Voldoire et al, 2013). In its reference version the horizontal resolution is 1.5° for the atmosphere and 1° for the ocean. This version will be referred to as LR in the following. A high resolution (referred to as HROA) uses 0.5° in the atmosphere and 0.25° in the ocean. We will also consider a high resolution atmosphere-only version (referred to as HRA) with 0.5° in the atmosphere and 1° in the ocean. These three versions have been used to re-forecast the 1993-2009 period. There are four hindcasts per year, starting at the beginning of February, May, August and November, and ending seven months later. Each hindcast is based on 60 members, generated by small initial perturbations of the atmospheric state.

The ENSO phenomenon is measured by the mean monthly sea surface temperature in the 5°S-5°N by 170°W-120°W rectangle (Nino3.4 box). Figure 1 shows the time correlation, based on 17 observed-predicted pairs, as a function of the lag for the 4 seasons. The impact of higher resolution is far from systematic, according to the season, with an improvement in Autumn, and a degradation in Spring.

The NAO is another large-scale phenomenon, but, contrary to ENSO, it has many temporal scales from the week to the decade. Here it is defined as the first EOF of the daily geopotential height over the rectangle 90W-30E 20N-80N for a given season. We address here the seasonal scale, by averaging months 2 to 4 of the forecasts. Only the DJF mean index exhibits a significant correlation between observation and forecast. Another difference with ENSO is that NAO is a chaotic phenomenon: within an ensemble, some members have a positive mean NAO, some have a negative one. So the NAO index within a season can be characterized by its pdf rather than by a single value. According to the limit central theorem, the mean NAO of a large ensemble (here 60 members) has a Gaussian pdf. One can therefore generate many NAO sequences for the 17 winters and calculate many NAO scores. We obtain thus a pdf for the NAO time correlation taking into account the sampling uncertainty of the ensemble. Figure 2 shows the pdf for the three versions. The mean correlation is 0.46 for LR, 0.51 for HROA, and 0.36 for HRA. The only significant difference is between HRA and HROA.

Additional experiments with 71 vertical levels instead of 31 in the atmosphere, with 3h coupling frequency instead of 24 h indicate that the absence of systematic jump in the forecast scores with high horizontal resolution is a robust characteristics of the model. These results, together with other forecast scores, which confirm this last feature, are available on SPECS Technical Report 1, which can be downloaded at:
http://www.specs-fp7.eu/SPECS/Technical_notes.html

Acknowledgements : We acknowledge that the results in this paper have been achieved using the PRACE Research Infrastructure resource Curie based in France at TGCC (project ID 2012060982). Scientific analyses and additional experiments have been carried in the framework of the FP7-SPECS project of the European Commission

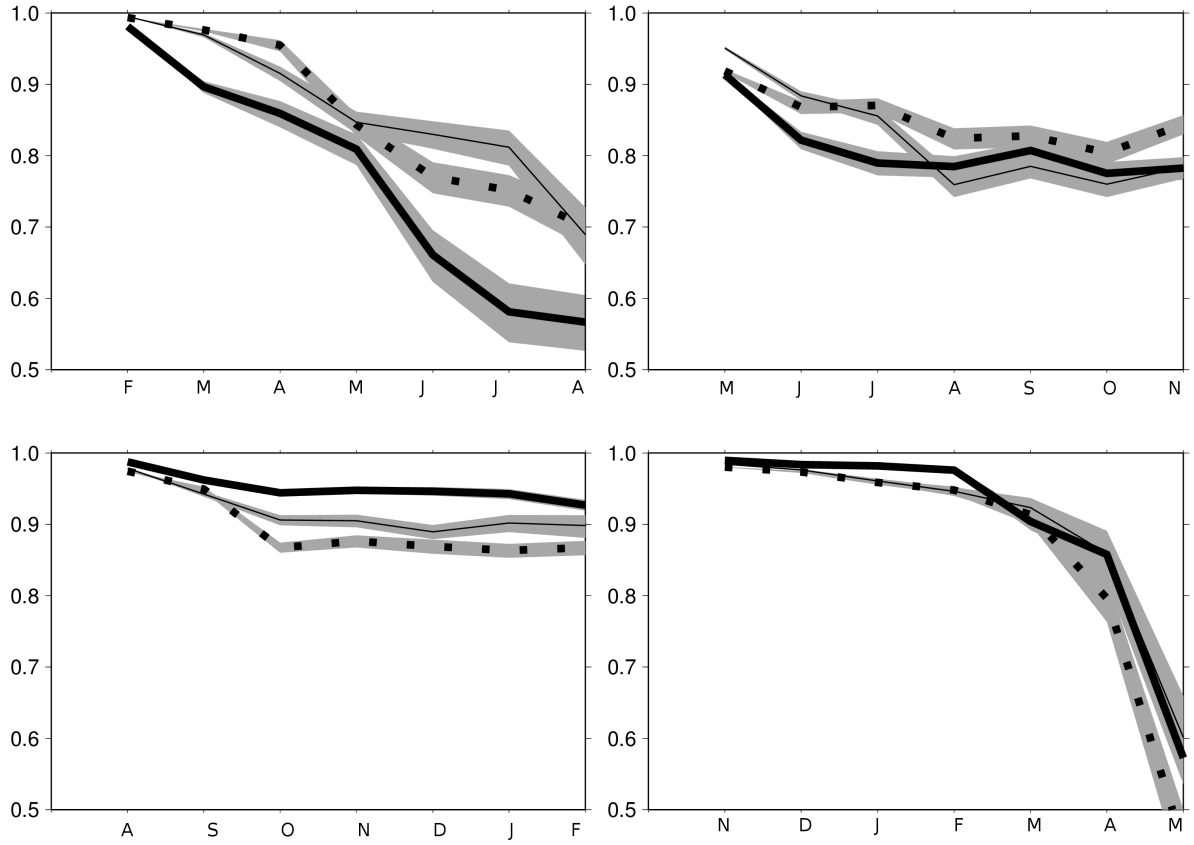

Figure 1: ENSO scores for the 4 seasons with LR (thin line), HROA (thick solid line) and HRA (thick dotted line). Shading for the 95% confidence intervals.

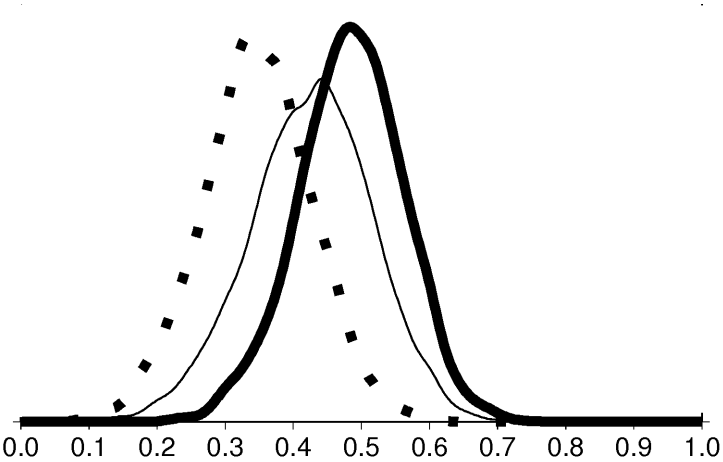

Figure 2: Probability density function for the NAO correlation coefficient in DJF: LR (thin line), HROA (thick solid line) and HRA (thick dotted line).

References:

Voldoire, A. E. Sanchez-Gomez, D. Salas y Mélia, B. Decharme, C. Cassou, S.Sénési, S. Valcke, I. Beau, A. Alias, M. Chevallier, M. Déqué, J. Deshayes, H. Douville, E. Fernandez, G. Madec, E. Maisonnave , M.-P. Moine, S. Planton, D. Saint-Martin, S. Szopa, S. Tyteca, R. Alkama, S. Belamari, A. Braun, L. Coquart, F. Chauvin., 2013, The CNRM-CM5.1 global climate model : description and basic evaluation , Clim. Dyn., DOI:10.1007/s00382-011-1259-y, online.

Upgrade of JMA's Typhoon Ensemble Prediction System

Masakazu Higaki, Masayuki Kyouda, Haruki Yamaguchi
Numerical Prediction Division, Japan Meteorological Agency
e-mail: m-higaki@naps.kishou.go.jp

1. Introduction

Since February 2008, the Japan Meteorological Agency (JMA) has operated its Typhoon Ensemble Prediction System (TEPS) designed to improve track forecast targeting for tropical cyclones (TCs) in the Regional Specialized Meteorological Center (RSMC) Tokyo - Typhoon Center's area of responsibility within the framework of the World Meteorological Organization. The forecast model employed in TEPS is a low-resolution version of JMA's Global Spectral Model (GSM). A singular vector (SV) method is adopted in TEPS to generate its initial perturbations, and dry SVs targeting the mid-latitude area are calculated for the Center's area of responsibility. The system also calculates moist SVs targeting TC surroundings where moist processes are critical. A stochastic physics scheme is used in TEPS in consideration of model uncertainties associated with physical parameterizations. JMA published a detailed description of its EPS suite including TEPS in 2013 (see reference).

2. Major upgrade of JMA's TEPS in March 2014

A major upgrade of JMA's TEPS was implemented in March 2014. The improvement included enhancement for the horizontal resolution of the forecast model from TL319 to TL479, revision of its physical processes (such as the stratocumulus and radiation schemes) and an ensemble size increase to 25. The major differences between the previous and upgraded TEPSs are listed in Table 1.

Table 1: Major upgrades applied to JMA's Typhoon EPS in March 2014

	Previous system	Upgraded system
Forecast model version	GSM1011	GSM1304 - Upgraded stratocumulus scheme - Upgraded radiation scheme
Horizontal resolution	TL319 (approx. 55 km)	TL479 (approx. 40 km)
Time step	1,200 sec.	720 sec.
Ensemble size	11 (Control run + 10 perturbed runs)	25 (Control run + 24 perturbed runs)
Perturbation generator	Singular vector method (SV)	SV with reduced initial spread

3. Impact of each enhancement on typhoon forecasting

A preliminary experiment involving the use of TEPS with the TL479-version GSM was conducted to investigate the impact of a higher-horizontal-resolution model on typhoon forecasting. The results showed that the higher-resolution TEPS supported sharper representation of TCs than the previous TEPS not only for typhoon-category storms but for all tropical depressions. The error of TC tracks predicted using the higher-resolution TEPS was also smaller than that of the previous TEPS, mainly due to the reduction of systematic biases.

In order to investigate the impact of a larger ensemble size on probabilistic TC track forecasting, another experimental configuration in which the ensemble initial conditions were increased from 11 to 25 was tested. Comparison of Brier skill scores (BSSs) for TC strike probabilities showed higher values from the experiment than for the previous TEPS, indicating that

the ensemble size increase in the order of a dozen was associated with a higher level of skill. However, the enhancement produced excessive ensemble spread, causing negative impacts on ensemble TC track forecasting such that the initial ensemble spread needed to be reduced. Accordingly, initial perturbation with a reduced amplitude was applied to TEPS. The results of another experiment after the revision indicated that the reduced amplitude provided better performance in combination with the increased ensemble size.

4. Performance of the upgraded TEPS

An experiment was conducted for the period from 2011 to 2013 on the upgraded TEPS before it was put into operation. The verification period included 2,056 TC forecasts over the northwestern Pacific in 1,527 TEPS runs. Figure 1 illustrates the position errors of the ensemble mean tracks derived from the previous and upgraded TEPSs, and shows that those of the latter were significantly smaller. The probabilistic verification results for the upgraded TEPS are also better than those for the previous TEPS (Figure 2). These outcomes indicate that the upgrade increased the appropriateness of the ensemble spread and improved TC track forecast skill.

REFERENCE

Japan Meteorological Agency, 2013: Outline of the operational numerical weather prediction at the Japan Meteorological Agency (JMA). Appendix to the WMO Technical Progress Report on the Global Data-Processing and Forecasting System and Numerical Weather Prediction, JMA. 188pp.

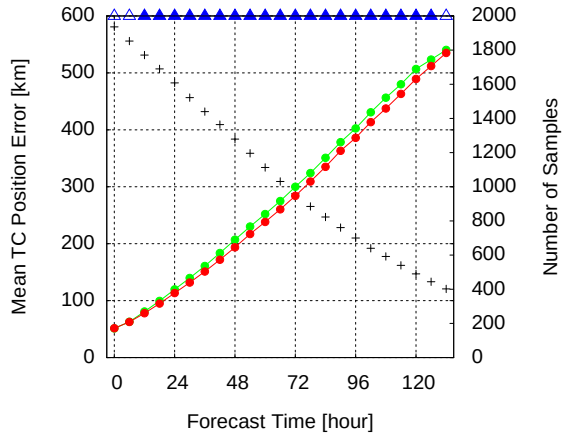

Figure 1: Mean position errors of ensemble mean TC tracks. Verified samples are all from TCs over the northwestern Pacific from 2011 to 2013. The horizontal axis shows the forecast range up to 132 hours ahead, and the green and red lines represent the results of verification for the previous and upgraded Typhoon EPSs, respectively. Plus marks indicate the numbers of verified samples based on the vertical scale on the right. The filled (open) triangles indicate that the differences of the two EPS results are statistically significant (insignificant) at a 95% confidence level.

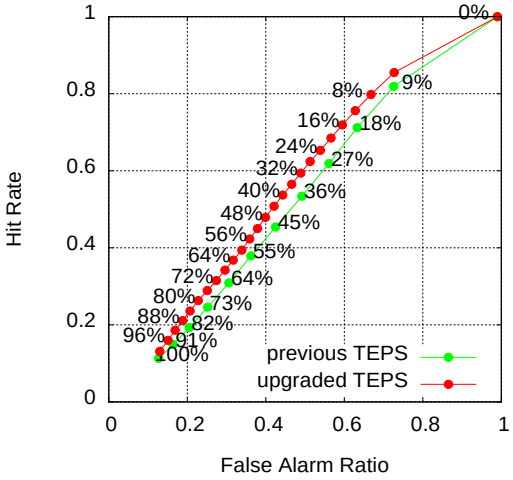

Figure 2: Probability of detection (POD) as a function of the false alarm ratio (FAR) for TC strike probability, defined as the fraction of ensemble members passing within 120 km of a given location in a five-day period. Verified samples are all from TCs over the northwestern Pacific from 2011 to 2013. The green and red lines represent the results of verification for ensemble TC tracks derived from the previous and upgraded Typhoon EPSs, respectively.

March 2014 upgrade of JMA's One-month Ensemble Prediction System

Masayuki Hirai*, Kengo Miyaoka, Hitoshi Sato, Hiroyuki Sugimoto, Atsushi Minami, Chihiro Matsukawa
Climate Prediction Division, Japan Meteorological Agency (JMA)
(E-mail: m-hirai @ met.kishou.go.jp)

Introduction

JMA's Ensemble Prediction System (EPS) for operational one-month forecasting (referred to here as the One-month EPS) employs an atmospheric global circulation model (AGCM). JMA implemented a major upgrade of the One-month EPS on 6 March 2014. The main changes are described below.

Main changes

(1) Improvement of the AGCM

The AGCM used for the One-month EPS is a lower-resolution version of JMA's Global Spectral Model (GSM) for short-range deterministic prediction. With the One-month EPS upgrade, the AGCM's horizontal resolution was increased from TL159 (110 km) to TL319 (55 km). Its version was also upgraded from GSM1011 to GSM1304 to include changes in certain physical processes such as stratocumulus parameterization (Shimokobe 2012).

(2) Improvement of AGCM boundary conditions

The horizontal resolution of sea surface temperature (SST) and sea ice distribution for the lower boundary conditions of the AGCM was increased using Merged satellite and in situ data Global Daily Sea Surface Temperature data (MGDSST; JMA 2013) and sea ice concentration data with a higher resolution (0.25 x 0.25 degrees) than that for previous SST and ice data (COBE-SST; 1.0 x 1.0 degrees; Ishii et al., 2005).

Prescribed sea ice distribution estimated using initial anomalies of sea ice distribution and statistics on the frequency of sea ice presence was also applied (Sugimoto and Takaya 2013) in order to produce results more appropriate than those calculated using climatological distribution only.

(3) Improvement of ensemble method

A stochastic physics scheme designed in consideration of model uncertainties associated with physical parameterization was introduced (Buizza et al. 1999; Yonehara and Ujiie 2011).

The results of a full set of hindcasts executed using the new system indicated enhanced prediction skill. For details, see Sato et al. (2014) in Section 6 of this issue.

Table 1 Specifications of JMA's old and new one-month EPSs

		Old system (operated until Feb. 2014) V1103	New system (from Mar. 2014) V1403
Model	Atmospheric model (version)	JMA's Global Spectral Model (GSM 1011)	JMA's Global Spectral Model (GSM 1304)
	Resolution	Horizontal: TL159 (approx. 1.125°) Vertical: 60 levels up to 0.1 hPa	Horizontal: TL319 (approx. 0.5625°) Vertical: 60 levels up to 0.1 hPa
Boundary condition	Sea surface temperature	Persisted anomaly with COBE-SST (1.0° x 1.0°)	Persisted anomaly with MGDSST (0.25° x 0.25°)
	Sea ice	Climatology of sea ice analysis (1.0° x 1.0°)	Prescribed sea ice distribution estimated using initial anomalies of sea ice (0.25° x 0.25°)
Ensemble method	Initial perturbation method	Combination of: - Breeding of Growing Modes (BGM) - Lagged Average Forecast (LAF) (25 BGMs and 2 initial dates with 24-hour LAF)	
	Model ensemble method	None	Stochastic physics scheme
	Ensemble size	50	
Operation	Initial time	12 UTC on Wednesday and Thursday	12 UTC on Tuesday and Wednesday
	Forecast range	816 hours (34 days)	

References

Buizza, R., M. Miller, and T. N. Palmer, 1999: Stochastic representation of model uncertainties in the ECMWF Ensemble Prediction System. *Quart. J. Roy. Meteor. Soc.*, **125**, 2887-2908.

JMA, 2013: Merged satellite and in-situ data global daily sea surface temperature. *Outline of the operational numerical weather prediction at the Japan Meteorological Agency. Appendix to WMO Technical Progress Report on the Global Data-processing and Forecasting Syste*m *(GDPFS) and Numerical Weather Prediction (NWP) Research*, Japan Meteorological Agency, Tokyo, Japan, 138. Available online at http://www.jma.go.jp/jma/jma-eng/jma-center/nwp/outline2013-nwp/index.htm.

Sato, H. and coauthors, 2014: Performance of JMA's new One-month Ensemble Prediction System. CAS/JSC WGNE Research Activities in Atmospheric and Oceanic Modelling, submitted.

Shimokobe, A., 2012: Improvement of the Stratocumulus Parameterization Scheme in JMA's Operational Global Spectral Model. *CAS/JSC WGNE Res. Activ. Atmos. Oceanic Model.*, **42**, 4.17-18.

Sugimoto, H. and Y. Takaya, 2013: A Method of Predicting Sea Ice Boundary Conditions for the One-month Ensemble Prediction System, *CAS/JSC WGNE Res. Activ. Atmos. Oceanic Model.*, **43**, 6.13-14.

Yonehara, H. and M. Ujiie, 2011: A Stochastic physics scheme for model uncertainties in the JMA one-week Ensemble Prediction System, *CAS/JSC WGNE Res. Activ. Atmos. Oceanic Model.*, **41**, 6-9-10.

The Evaluation of the Vertical Structures of Marine Boundary Layer Clouds over Mid-Latitudes

Hideaki Kawai[1] (h-kawai@mri-jma.go.jp), **Syoukichi Yabu[1]**, **Yuichiro Hagihara[2]**
[1]*Meteorological Research Institute, Japan Meteorological Agency*
[2]*Kyushu University, Fukuoka, Japan*

1. Introduction

Mid-latitude marine low clouds are not adequately represented in the operational global model of the Japan Meteorological Agency (JMA); i.e., the GSM (Global Spectral Model). In order to understand the faults in the physical processes related to the mid-latitude marine low clouds in the models, the characteristics of such clouds in the model should be evaluated in detail from many perspectives using observational data. Here, we examine the vertical structures of such clouds using cloud mask data, which were retrieved from CloudSat and CALIPSO.

The structures of mid-latitude marine low clouds have not been investigated as intensively as have subtropical ones. One of the reasons is that evaluation for mid-latitude low clouds is more difficult than that for subtropical low clouds because high or middle clouds often prevail in the mid-latitudes. Moreover, comparison of low clouds represented in GCMs with those from observational data is complicated by the need for an overlap assumption. Therefore, the influence of upper-level clouds is minimized by considering only the low cloud top area, and the impact of the overlap assumptions on the evaluation is also examined, in this study.

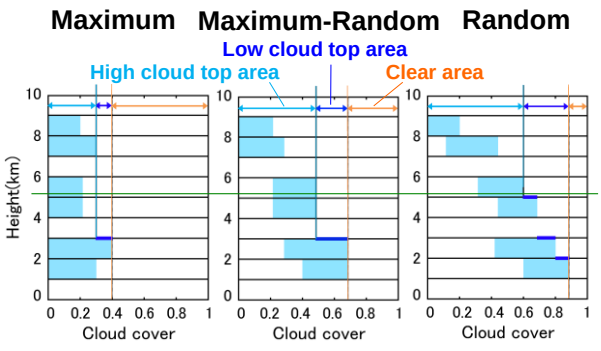

Fig. 1: Schematic diagrams showing three cloud overlap assumptions tested in this study (left: maximum overlap, middle: maximum-random overlap, right: random overlap), which are modified from Hogan and Illingworth (2000). The light blue double-headed arrows correspond to high cloud top area, blue to low cloud top area, and orange to clear area.

2. Data and the Processing

2.1. Observation data

The Kyusyu University cloud mask data (Hagihara et al. 2010), which were retrieved from CloudSat and CALIPSO and have a vertical resolution of 240 m and a horizontal resolution of 1.1 km, were used in the comparison ("CloudSat or CALIPSO mask (C4) data" were used). The data were excluded from the statistical analysis if there were clouds present above 5 km, because the target of this study is low clouds not covered by upper-level clouds (higher than 5 km), which are important for global radiation budget.

2.2. Model data

The original vertical level data (TL159L60) from the simulation using the model are used for the comparison. Three different assumptions related to cloud overlap (Fig. 1) are tested (note that the maximum-random overlap is used in the radiation process in the JMA-GSM). The occurrence frequency of cloud top height (CTH) is normalized by the low (lower than 500 hPa) cloud top area (blue arrow areas in Fig. 1). CTH data in model grids with no or little upper-level cloud cover (higher than 500 hPa) are selected and used.

3. Results

Figure 2 shows the results of the comparison. The characteristics of the CTH in the mid-latitudes from the observations are presented and discussed in detail in Kawai et al. (2014), and we briefly summarize the results of the comparison between the observations and the model in this report.

Over the North Pacific, the observed CTH is remarkably high (ca. 2 km) in winter and clearly low (ca. 500 m) in summer around 40°–55°N. The amplitude of the seasonal variation simulated by the model is smaller than that observed. In particular, the CTH in winter is much lower in the model than that observed.

Over the Southern Ocean, the observed CTH is higher in winter around 40°–55°S than in summer. Although the model represents this seasonal variation to some extent, CTH in the model is lower than that observed. The southward increase in CTH is found in summer in the observations but is not clear in the model, although the model captures low CTH around

40°–45°S. In winter, the lower CTH observed around 60°–65°S, possibly corresponding to the area of sea ice, is qualitatively represented in the model.

Figure 2 also shows that the difference in CTH distribution among different overlap assumptions is smaller than the systematic differences between the model and observations. The maximum overlap and the maximum-random overlap assumptions provide similar results. The random overlap assumption gives a wider distribution of CTH compared with the other assumptions.

Mid-latitude marine low clouds in the model capture the characteristics of CTH in nature to some extent. However, the comparison of the model with observations shows several significant differences, and the comparison result could help us to improve the parameterization and representation of clouds in the model.

Acknowledgements

This work was partly supported by the Research Program on Climate Change Adaptation (RECCA) of the Ministry of Education, Culture, Sports, Science and Technology (MEXT), Japan, and the "Program for Risk Information on Climate Change".

References

Hogan, R. J. and A. J. Illingworth, 2000: Deriving cloud overlap statistics from radar. *Q.J.R. Meteorol. Soc.*, **126**, 2903–2909.

Hagihara, Y., H. Okamoto, and R. Yoshida, 2010: Development of a combined CloudSat-CALIPSO cloud mask to show global cloud distribution. *J. Geophys. Res.*, **115**, D00H33, doi:10.1029/2009JD012344.

Kawai, H., S. Yabu, Y. Hagihara, T. Koshiro, and H. Okamoto, 2014: Characteristics of the Vertical Structures of Marine Boundary Layer Clouds over Mid-Latitudes. submitted.

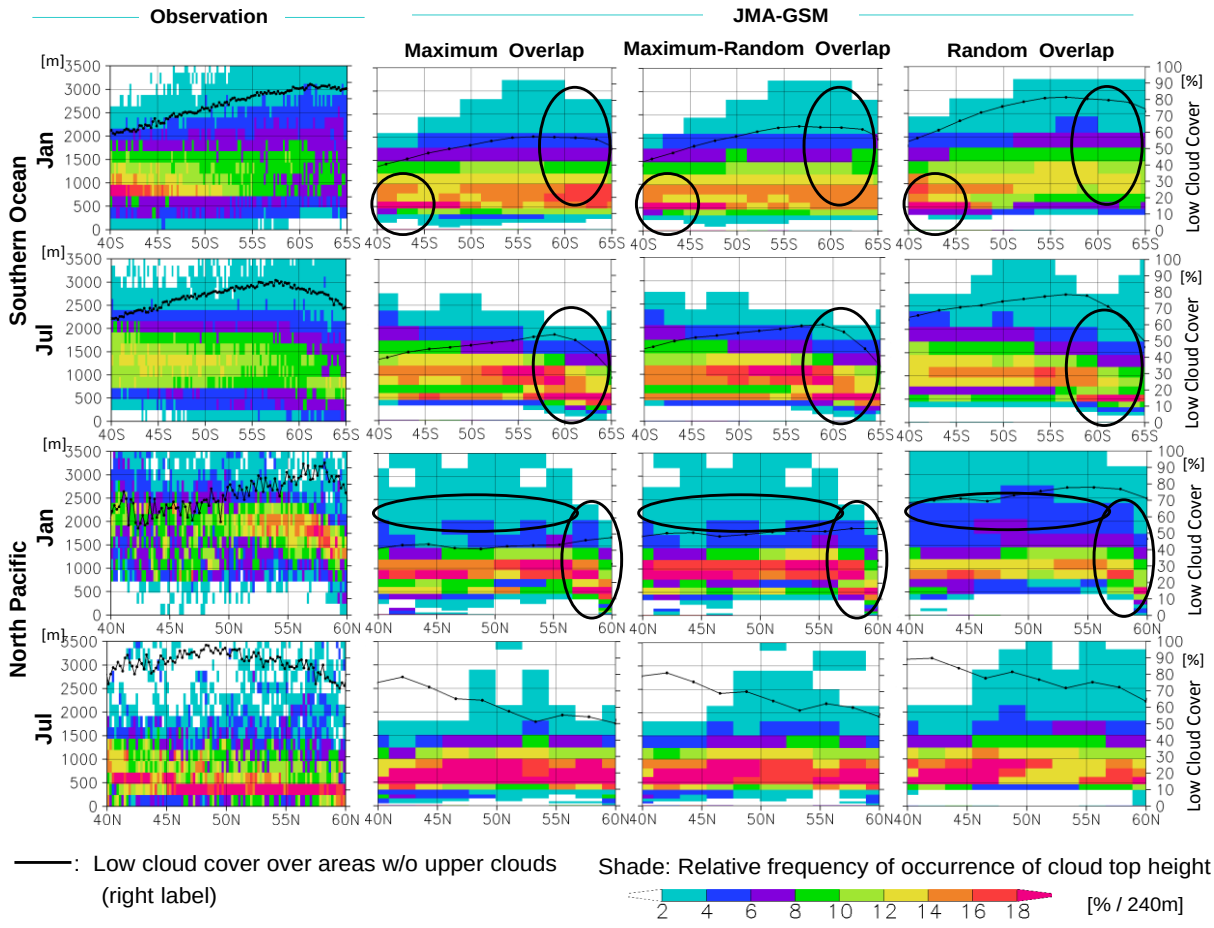

Fig. 2: Relative frequency of occurrence of cloud top height (CTH), which is normalized by the low cloud top area and the 240 m vertical bin, from observational data (left) and from simulations by the JMA-GSM (others). Three different overlap assumptions are used (second from left: maximum overlap, third from left: maximum-random overlap, fourth from left: random overlap). Black lines show low cloud cover over areas with no upper-level clouds. Three-year climatologies for January and July over the Southern Ocean (0°−360°) and over the North Pacific (165°E−165°W) are shown.

Performance of JMA's new One-month Ensemble Prediction System

Hitoshi Sato, Ryoji Nagasawa, Kengo Miyaoka, Masayuki Hirai, Yuhei Takaya,
Satoko Matsueda, Akihiko Shimpo, Hiroyuki Sugimoto
Climate Prediction Division, Japan Meteorological Agency, Tokyo, Japan
(E-mail: sato.hitoshi@met.kishou.go.jp)

1. Introduction

The Japan Meteorological Agency (JMA) upgraded its operational One-month Ensemble Prediction System (EPS) in March 2014 (for details, see Hirai et al. 2014). The main changes include a horizontal resolution increase from TL159 to TL319, a revision of the SST/sea-ice specifications prescribed as lower boundary conditions, and the introduction of a stochastic physics scheme.

The performance of the new One-month EPS (referred to here as V1403) was evaluated via hindcast experiments carried out for the 30-year period from 1981 to 2010.

2. Hindcast experiments

Atmospheric and land initial conditions for the experiments conducted with V1403 were provided from the Japanese 55-year Reanalysis (JRA-55; Ebita et al. 2011), which is the latest atmospheric reanalysis dataset produced by JMA. In contrast, those for the experiments conducted with the previous EPS (V1103) were provided from JRA-25/JCDAS (Onogi et al. 2007). A summary of the experiments is given in Table 1.

3. Verification results

The impact on one-month forecast skill scores was examined based on the outcomes of the hindcast experiments. The anomaly correlation for 30-day mean 500-hPa geopotential height (Z500) during boreal winter (December – February) shown in Figure 1 suggests an improvement for most parts of the extratropics. V1403 has a positive impact on skill scores for most variables in all regions and forecast ranges. Significant improvement is seen in the early forecast range (Figure 2).

The bias of the 28-day mean Z500 in the Northern Hemisphere (20˚N – 90˚N) during boreal winter is shown in Figure 3. Although the spatial pattern of the bias is similar with both V1103 and V1403, its magnitude with V1403 is reduced for most parts of the Northern Hemisphere, especially over northern Europe. Model biases in the extratropics are generally improved, while the impact on biases in the tropics is relatively small. For the Asian summer monsoon, the weaker circulation bias is strengthened in V1403.

The new configuration's capacity to represent atmospheric phenomena was verified. The frequency of blocking is underestimated (particularly in the Euro-Atlantic sector) with V1103, while the frequency of wintertime blocking in the sector is increased with V1403 (for details, see Shimpo 2014).

The impact on synoptic eddy activity based on 10-day high-pass filtered wind at 300 hPa is positive, with improvement of overly weak eddy activity in the extratropics.

Madden-Julian oscillation (MJO) prediction skill was assessed using the method detailed by Matsueda and Takaya (2012). The results suggested a neutral impact on MJO forecast skill and a slightly negative impact on MJO amplitude (i.e., smaller values).

4. Conclusions

The impact of the new One-month EPS on forecast skill was verified using hindcast experiments. Forecast skill scores showed significant improvement, especially in the early forecast range. Model biases are generally reduced in the extratropics, while the impact on biases in the tropics is relatively small. Representation of blocking frequency and synoptic eddy activity in the extratropics is also improved, while the impact on MJO prediction ability is close to neutral.

References

Ebita, A. and coauthors, 2011: The Japanese 55-year Reanalysis "JRA-55": an interim report. *SOLA*, **7**, 149-152.

Hirai, M. and coauthors, 2014: March 2014 upgrade of JMA's One-month Ensemble Prediction System. *CAS/JSC WGNE Research Activities in Atmospheric and Oceanic Modelling*, submitted.

Matsueda, S. and Y. Takaya, 2012: Forecast skill of MJO with the JMA's One-month Ensemble Prediction System. CAS/JSC WGNE Res. Activ. Atmos. Oceanic Model., **42**, 6.11-12.

Onogi, K. and coauthors, 2007: The JRA-25 Reanalysis. *J. Meteor. Soc. Japan*, **85**, 369-432.

Shimpo, A., 2014: Climatological wintertime blocking frequency for the Northern Hemisphere in JMA's new One-month Ensemble Prediction System. *CAS/JSC WGNE Research Activities in Atmospheric and Oceanic Modelling*, submitted.

Table 1 Specifications of one-month hindcast experiments

	V1103 (operated until February 2014)	V1403 (since March 2014)
Atmospheric model	GSM 1011	GSM 1304
Resolution (model top)	TL159 L60 (0.1 hPa)	TL319 L60 (0.1 hPa)
Initial conditions Atmosphere Land surface	 JRA-25/JCDAS Climatology	 JRA-55 JRA-55
SST	COBE-SST, persisted anomaly	MGDSST, persisted anomaly
Sea ice distribution	Climatology	Statistical prediction
Ensemble method	Breeding of Growing Modes (BGM)	BGM + Stochastic physics scheme
Ensemble size	5	
Period	1981 – 2010 (3 initial dates a month)	
Verification data	JRA-55	

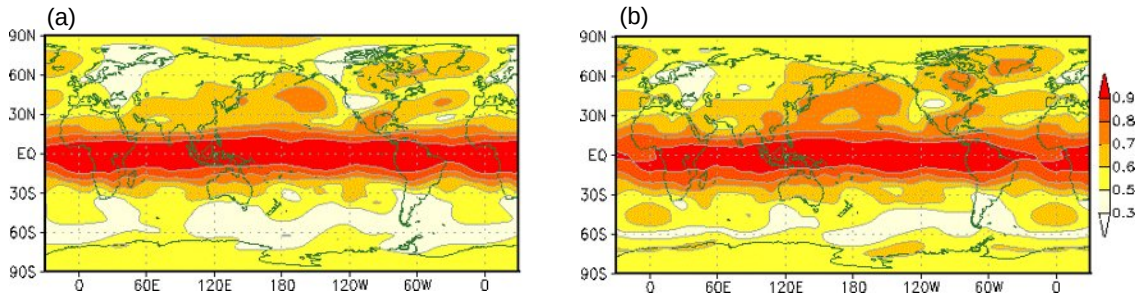

Figure 1 Anomaly correlation of 30-day (days 1 – 30) mean 500-hPa geopotential height for boreal winter during the period from 1981 to 2010 with (a) V1103 and (b) V1403

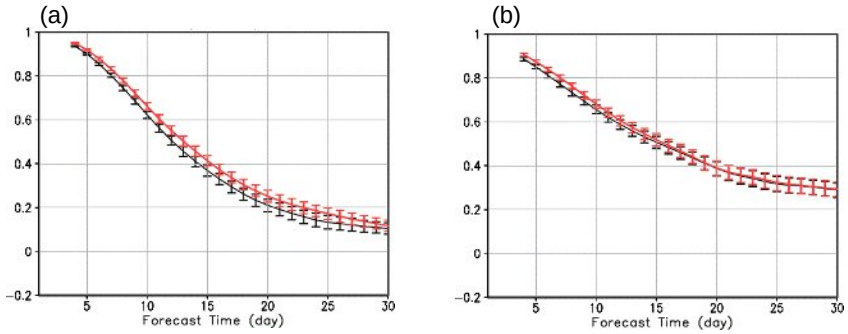

Figure 2 Anomaly correlation of (a) 500-hPa geopotential height in the Northern Hemisphere (20˚N – 90˚N) and (b) mean sea level pressure in the tropics (20˚S – 20˚N) for boreal winter during the period from 1981 to 2010. Scores are based on seven-day mean fields with V1103 (black) and V1403 (red). The vertical bars indicate 95% confidence intervals.

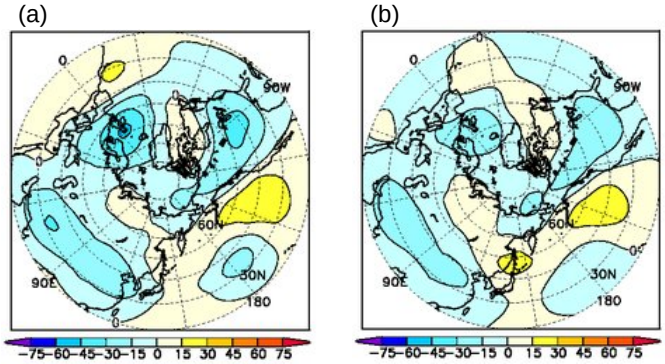

Figure 3 Bias of 28-day (days 3 – 30) mean 500-hPa geopotential height (m) for boreal winter during the period from 1981 – 2010 with (a) V1103 and (b) V1403

Climatological wintertime blocking frequency for the Northern Hemisphere in JMA's new One-month Ensemble Prediction System

Akihiko Shimpo
Climate Prediction Division, Japan Meteorological Agency, Tokyo, Japan
(E-mail: sinpo @ met.kishou.go.jp)

1. Introduction

As atmospheric blocking (referred to here simply as *blocking*) has a significant impact on regional climatic conditions, the capacity for its representation in Numerical Weather Prediction (NWP) modeling is very important. In this study, climatological wintertime blocking frequency for the Northern Hemisphere in the new Japan Meteorological Agency (JMA) One-month Ensemble Prediction System (EPS) was investigated based on related hindcast (re-forecast) experiments.

2. Data and method

JMA plans to upgrade its One-month EPS in March 2014 (Hirai et al. 2014). The new EPS (referred to here as V1403) has a horizontal resolution of TL319 (55km), which is higher than the TL159 (110km) specification of the old version (V1103) operated until February 2014. As a result, blocking frequency improvement is expected (e.g., Matsueda et al. 2009; Jung et al. 2012). Data sets from hindcast experiments for V1403 and V1103 are available for the 30-year period from 1981 to 2010 (Sato et al. 2014) and the Japanese 55-year Reanalysis (JRA-55; Ebita et al. 2011) is used for analysis data. In this study, blocking frequencies were investigated for 29 boreal winters (December, January, February, or DJF) in the period from 1981/1982 to 2009/2010 with five-member ensembles. Regarding the configuration of the hindcast experiments, predictions made during the period from 4 to 31 days ahead and started on ten initial dates between 10th November and 20th February (every ten days or so) were used.

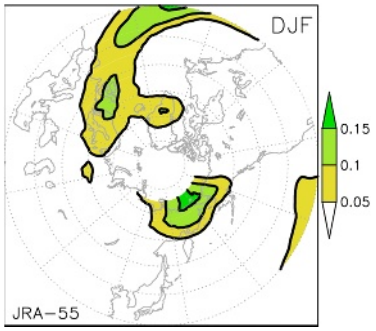

Figure 1 Climatological blocking frequency in analysis (JRA-55) in boreal winter (DJF)
Contour interval is 0.05 and the lowest contour is 0.05. Climatology is calculated from 29 years from 1981/1982 to 2009/2010.

Blocking was assessed using an index calculated from seven-day running means of daily 500hPa geopotential height (Z500) based on the method of Scherrer et al. (2006), which is an extension from the approach proposed by Tibaldi and Molteni (1990) (referred to here as TM90). A grid was considered to be blocking when the conditions below were satisfied with latitude ϕ and $\Delta\phi = 15\mathrm{degs}$.

$$GHGS = [Z500(\phi) - Z500(\phi + \Delta\phi)]/\Delta\phi > 0$$
$$GHGN = [Z500(\phi - \Delta\phi) - Z500(\phi)]/\Delta\phi < -10[m/deg]$$

3. Results

Figure 1 shows wintertime (DJF) blocking frequency derived with JRA-55 data used for the analysis fields. In the mid- and high-latitudes, two major peaks are present in the Euro-Atlantic and Pacific sectors, which is consistent with the outcomes of many previous studies (e.g., TM90; Scherrer et al. 2006). Figure 2 shows the predicted blocking frequencies of V1403 and V1103 and their differences from that of the analysis, and also indicates the difference between V1403 and V1103.

In the Euro-Atlantic sector, the blocking frequencies of V1403 and V1103 are both lower than that of the analysis. However, the blocking frequency deficiency in V1403 is smaller than that in V1103, which means the frequency is increased and improved in V1403. This is clearly seen in the longitudinal distribution of blocking frequency at 60°N, which is consistent with TM90, except in the latitudinal band ranges 5° north and south of 60°N (Figure 3).

In the Pacific sector, meanwhile, the blocking frequency deficiency in V1403 is stronger than that of V1103. Blocking frequency dependency on lead time in V1103 is stronger than that in V1403, and as a result, the blocking frequency in V1103 over the Pacific sector averaged for all lead times appears similar to that of the analysis (not shown). This weakening of lead time dependency in V1403 can be seen as an improvement, though a deficiency compared to the analysis remains.

4. Summary

In this study, climatological blocking frequencies in JMA's One-month EPS were investigated using data sets from related hindcast experiments and compared to analysis derived from JRA-55. It was found that the new EPS (V1403) shows improved climatological wintertime blocking frequency for the Northern Hemisphere. As V1403 has a higher horizontal resolution than the old version (V1103), this result is consistent with those of previous studies (e.g., Matsueda et al. 2009; Jung et al. 2012). However, blocking frequency in V1403 was still deficient in comparison to the analysis results, which is also consistent with the tendency seen in JMA's One-week EPS (Matsueda 2008). To clarify the model's capacity for blocking representation, more detailed investigation is needed such as the persistency of blocking and interannual variations of blocking frequency in the model.

Reference

Ebita, A., S. Kobayashi, Y. Ota, M. Moriya, R. Kumabe, K. Onogi, Y. Harada, S. Yasui, K. Miyaoka, K. Takahashi, H. Kamahori, C. Kobayashi, H. Endo, M. Soma, Y. Oikawa, and T. Ishimizu, 2011: The Japanese 55-year Reanalysis "JRA-55": an interim report, *SOLA,* **7,** 149-152.

Hirai, M., and coauthors, 2014: March 2014 upgrade of JMA's One-month Ensemble Prediction System. *CAS/JSC WGNE Research Activities in Atmospheric and Oceanic Modelling,* submitted.

Jung, T., M. J. Miller, T. N. Palmer, P. Towers, N. Wedi, D. Achuthavarier, J. M. Adams, E. L. Altshuler, B. A. Cash, J. L. Kinter III, L. Marx, C. Stan, and K. I. Hodges, 2012: High-Resolution Global Climate Simulations with the ECMWF Model in Project Athena: Experimental Design, Model Climate, and Seasonal Forecast Skill. *J. Climate,* **25,** 3155-3172.

Matsueda, M., 2008: Blocking Predictability in Operational Medium-Range Ensemble Forecasts. *SOLA,* **5,** 113–116.

Matsueda, M., R. Mizuta, and S. Kusunoki, 2009: Future change in wintertime atmospheric blocking simulated using a 20-km-mesh atmospheric global circulation model. *J. Geophys. Res.,* **114,** D10114, doi:10.1029/2007JD009647.

Sato, H., and coauthors, 2014: Performance of the JMA's new One-month Ensemble Prediction System. *CAS/JSC WGNE Research Activities in Atmospheric and Oceanic Modelling,* submitted.

Scherrer, S. C., M. Croci-Maspoli, C. Schwierz, and C. Appenzeller, 2006: Two-dimensional indices of atmospheric blocking and their statistical relationship with winter climate patterns in the Euro-Atlantic region, *Int. J. Climatol.,* **26,** 233-249.

Tibaldi, S., and F. Molteni, 1990: On the operational predictability of blocking. *Tellus,* **42A,** 343-365.

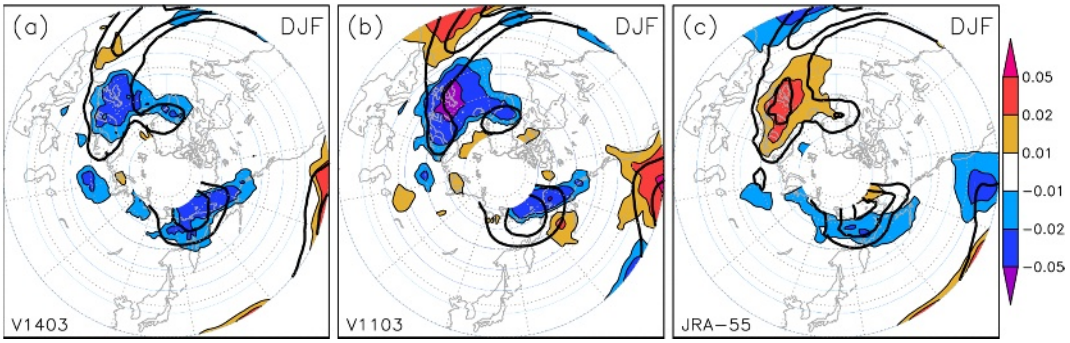

Figure 2 Climatological blocking frequency in JMA's One-month EPS in boreal winter (DJF)
(a) V1403 (contour) and related differences from the analysis (shaded). (b) As per (a), but for V1103. (c) Analysis (JRA-55; contours as per Figure 1) and differences between V1403 and V1103 (V1403 - V1103; shaded). The contour interval is 0.05 and the lowest contour is 0.05. Shading is as shown in the color bar index. The climatology is calculated for the 29-year period from 1981/1982 to 2009/2010.

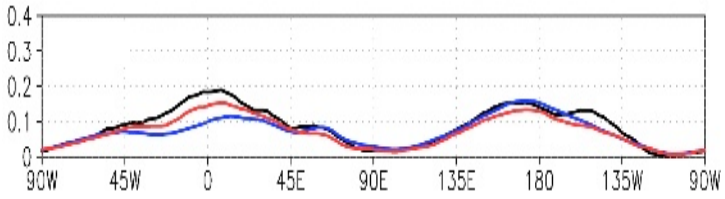

Figure 3 Longitudinal distribution of climatological blocking frequency in boreal winter (DJF) at 60˚N
Analysis (JRA-55; black), V1403 (red), and V1103 (blue).

Upgrade of JMA's One-Week Ensemble Prediction System

Haruki Yamaguchi, Masakazu Higaki, Masayuki Kyouda
Numerical Prediction Division, Japan Meteorological Agency
e-mail: kyouda@naps.kishou.go.jp

1. Introduction

The Japan Meteorological Agency (JMA) has operated its One-Week Ensemble Prediction System (WEPS) since March 2001 (JMA 2013). A major upgrade implemented in February 2014 included enhancement of the forecast model's horizontal resolution from TL319 to TL479 and revision of its physical processes, such as the stratocumulus and radiation schemes. It also included increased frequency of operation from once a day to twice a day and an approximate halving of each ensemble size from 51 to 27 so that the total ensemble size is now 54/day as opposed to 51/day. The major differences between the previous and upgraded WEPSs are listed in Table 1. This upgrade has had a positive impact on forecast scores for both ensemble mean and probabilistic forecasts, and is expected to enhance forecasts of severe weather caused by tropical cyclones and local phenomena.

Table 1: Major upgrades applied to JMA's One-Week EPS in February 2014

	Previous system	Upgraded system
Forecast model version	GSM1011	GSM1304 - Upgraded stratocumulus scheme - Upgraded radiation scheme
Horizontal resolution	TL319 (approx. 55 km)	TL479 (approx. 40 km)
Time step	1,200 sec.	720 sec.
Forecast range (initial time)	264 hours (12 UTC)	264 hours (00, 12 UTC)
Ensemble size	51 (51/day)	27 (54/day)

2. Performance of the upgraded WEPS

An experiment was conducted for the periods from December 2011 to February 2012 and from July to September 2012 on the upgraded WEPS before it was put into operation. Figure 1 illustrates the anomaly correlation coefficients for the 500-hPa geopotential height of the ensemble mean forecast for the Northern Hemisphere extra-tropics, and shows that the upgraded WEPS is superior to the previous version for almost whole forecast range. However, a negative impact caused by ensemble size reduction partially offsets the positive impact of the model upgrade in the longer forecast range. For the upgraded WEPS, doubling the ensemble size by combining the latest and previous ensemble forecasts results in better verification scores for some probabilistic forecasts than using latest forecasts alone in the longer forecast range (not shown).

Figure 2 illustrates control member position errors in typhoon track forecasts derived from the previous and upgraded WEPSs. The errors of the upgraded version are smaller, indicating better forecasts. The higher-resolution model can make the central pressure of forecast tropical cyclones (TCs) lower and closer to that of analyses, while a high-pressure bias still remains. The TC forecast improvement also appears in ensemble mean forecasts. The benefit of increased horizontal resolution is also seen in orographic precipitation data. This results in improved verification scores in forecasting to determine the probability of precipitation over Japan in winter, when the winter monsoon tends to bring orographic precipitation to the upwind side of the Japanese Archipelago. Figure 3 shows Brier skill scores (BSSs) for probabilistic forecasts of 24-hour cumulative

precipitation exceeding 1 mm verified against rain gauge observations in Japan during the period from December 2011 to February 2012. The values for the upgraded WEPS are higher than those of the previous WEPS over the whole forecast range.

REFERENCE

Japan Meteorological Agency, 2013: Outline of the operational numerical weather prediction at the Japan Meteorological Agency (JMA). Appendix to the WMO Technical Progress Report on the Global Data-Processing and Forecasting System and Numerical Weather Prediction, JMA. 188pp.

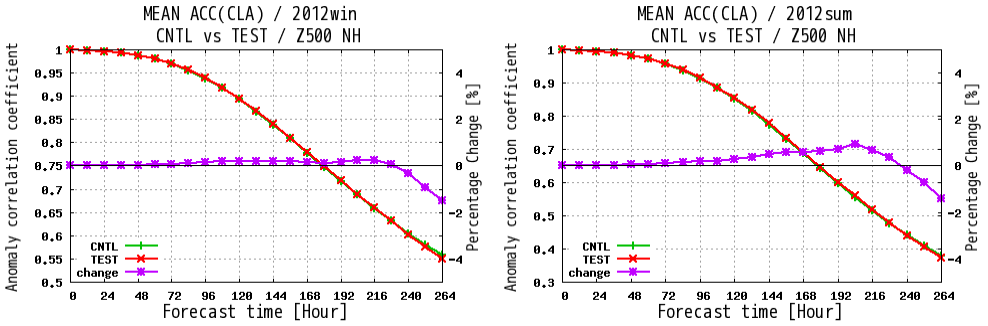

Figure 1: Anomaly correlation coefficients of 500-hPa geopotential height for ensemble mean forecasts from December 2011 to February 2012 (left) and from July to September 2012 (right). The horizontal axis shows the forecast range up to 264 hours ahead, and the green and red lines represent the results of verification for the previous and upgraded WEPSs, respectively. The purple line indicates the relative change (%) from the previous score to the upgraded score based on the vertical scale on the right; positive change means upgraded scores are higher than previous scores.

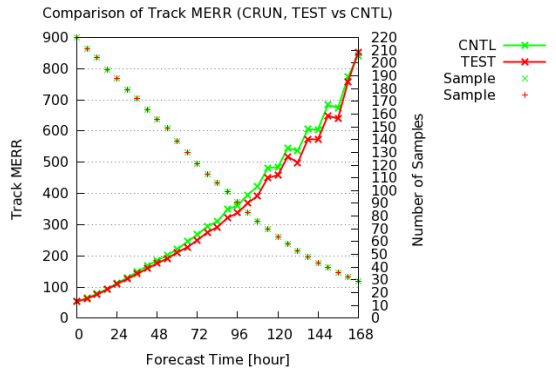

Figure 2: Mean position errors of control member TC tracks. Verified samples are all from TCs over the northwestern Pacific from July to September 2012. The horizontal axis shows the forecast range up to 168 hours ahead, and the green and red lines represent the results of verification for the previous and upgraded WEPSs, respectively. Plus marks indicate the numbers of verified samples based on the vertical scale on the right.

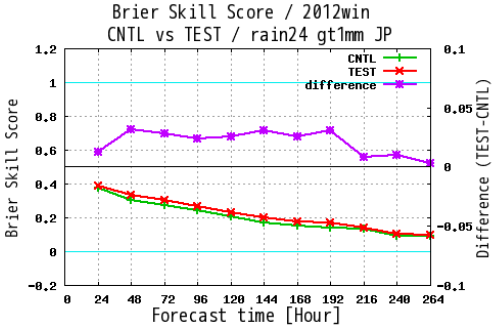

Figure 3: Brier skill scores for probabilistic forecasts of 24-hour cumulative precipitation exceeding 1 mm from December 2011 to February 2012 in Japan. The horizontal axis shows the forecast range up to 264 hours ahead, and the green and red lines represent the results of verification for the previous and upgraded WEPSs, respectively. The purple line indicates the difference calculated by subtracting the previous values from the upgraded values based on the vertical scale on the right.

Upgrade of JMA's Operational NWP Global Model

Hitoshi Yonehara, Masashi Ujiie, Takafumi Kanehama, Ryohei Sekiguchi, Yosuke Hayashi
Japan Meteorological Agency, Tokyo, Japan
(email: yonehara@naps.kishou.go.jp)

1. Introduction

In March 2014, the Japan Meteorological Agency (JMA) began operation of an upgraded Global Spectral Model (GSM: JMA 2013) with more vertical levels and a higher top level. The parameterization schemes for variables such as the boundary layer, radiation, non-orographic gravity waves and deep convection were also revised to improve the representation of atmospheric characteristics. This report briefly outlines the specifications of new vertical layers, parameterization improvements and verification results in relation to the upgrade.

2. Vertical layers

The number of vertical layers was increased from 60 to 100, and the pressure of the top level was raised from 0.1 hPa to 0.01 hPa. Table 1 compares the specifications of the new and old models, and Figure 1 compares their vertical layer distribution. The vertical resolution was increased at all elevations to reduce truncation errors caused by finite differentiation and to improve atmospheric vertical structure representation. In particular, more layers were applied mainly in the upper troposphere and the lower stratosphere to improve forecast accuracy for the troposphere and stratosphere, respectively. The main purposes of raising the model top were to allow the assimilation of more satellite observations with sensitivity for the middle atmosphere and to reduce the effect of pseudo-reflection from the model top in the stratosphere. In this connection, second-order linear horizontal diffusion was applied in the divergence equation and enhancement of fourth-order linear diffusion in the sponge layer around the model top was stopped.

3. Parameterization improvement

a. Boundary layer

Surface exchange coefficients based on the Monin-Obukhov similarity theory (Beljaars and Holtslag 1991) were introduced for bulk exchange formulation of land surface fluxes, and the vertical diffusive coefficients in the stable boundary layer were revised (Han and Pan 2011). These changes improved wind fields and diurnal cycles of temperature variation in stable conditions.

b. Radiation

A new long-wave radiation scheme based on a two-stream absorption approximation radiation transfer method (Yabu 2013) was introduced to improve the accuracy of the heating rate in the middle atmosphere and reduce computational cost. In the new long-wave radiation scheme, absorption relating to atmospheric molecules is calculated using a k-distribution approach. Despite the increased number of vertical levels, the computational cost of radiation was reduced.

Bare ground albedo parameter distribution was adopted instead of a globally uniform albedo, which substantially reduced mean errors of clear sky radiative fluxes near desert areas.

c. Gravity waves

Non-orographic spectral gravity wave forcing parameterization (Scinocca 2003) was introduced to replace Rayleigh friction in the forecast model in order to improve the middle atmospheric climate and representation of long-term oscillation (such as the quasi-biennial type) in the tropical lower stratosphere.

d. Deep convection

In the convection scheme, the energy correction method was adjusted to the new vertical levels. This mitigated extreme drying in the upper troposphere and improved large-scale circulation and precipitation distribution over the tropics.

4. Verification results

An experiment was conducted to evaluate the upgraded GSM's performance, including the impacts of improvements in data assimilation considerations such as the GNSS radio occultation bending angle (incorporating high-altitude data up to 0.1 hPa), AMSU-A 14 ch (with a sensitivity peak near 2 hPa) and ground-based GNSS zenith total delay. Although the revision of data assimilation and the increased number of vertical layers were not negligible, the parameterization improvements were the principal for forecast accuracy in the subsequent discussion.

Figure 2 shows profiles of mean errors (ME) and root mean square errors (RMSE) against the analysis for 11-day forecasting of geopotential height. The verification region is the whole globe, and the trial period is six months. The GSM improvements reduced ME and RMSE values for most pressure levels and all forecast times. Overall improvement was also found in forecasts of other elements such as global mean sea level pressure and 850/250-hPa vector wind in the extratropics.

Figure 3 shows that tropical cyclone track forecast errors for four regions are all reduced with the

upgraded GSM. Further verification indicates that the new model's performance for cyclone identification is better than that of the old version.

References

Beljaars, A. C. M. and A. A. M. Holtslag, 1991: Flux parameterization over land surfaces for atmospheric models. *J. Appl. Meteor.*, **30**, 327 – 341.

Japan Meteorological Agency, 2013: Outline of the Operational Numerical Prediction at JMA.

Jongil Han, Hua-Lu Pan, 2011: Revision of Convection and Vertical Diffusion Schemes in the NCEP Global Forecast System. *Wea. Forecasting*, **26**, 520 – 533.

Scinocca, J. F., 2003: An Accurate Spectral Non-orographic Gravity Wave Drag Parameterization for General Circulation Models. *J. Atmos. Sci.*, **60**, 667 –682.

Simmons, A. J. and D. M. Burridge, 1981: An energy and angular momentum conserving vertical finite difference scheme and hybrid vertical coordinates. *Mon. Wea. Rev.*, **109**, 758 – 766.

Simmons, A. J. and R. Strufing, 1983: Numerical forecasts of stratospheric warming events using a model with a hybrid vertical coordinate. *Q.J.R. Meteorol. Soc.*, **109**, 81 – 111.

Yabu, S. 2013: Development of longwave radiation scheme with consideration of scattering by clouds in JMA global model. *CAS/JSC WGNE Res. Activ. Atmos. Oceanic. Modell.*, **43**, 04.07 – 04.08.

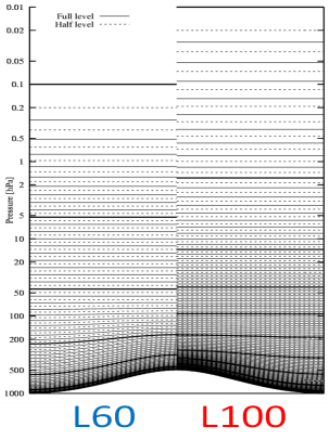

Fig. 1: Distribution of vertical layers: old model (left) and new model (right). The vertical coordinate system is based on Eta (sigma-p hybrid) coordinates (Simmons and Burridge 1981, Simmons and Strufing 1983) and the bottom half level is the surface. Solid and dashed lines show full and half levels, respectively.

Table 1: Model specifications

	Old	New
Horizontal resolution	TL959	
Vertical levels	60	100
Model top [hPa]	0.1	0.01
Time step [sec]	600	400

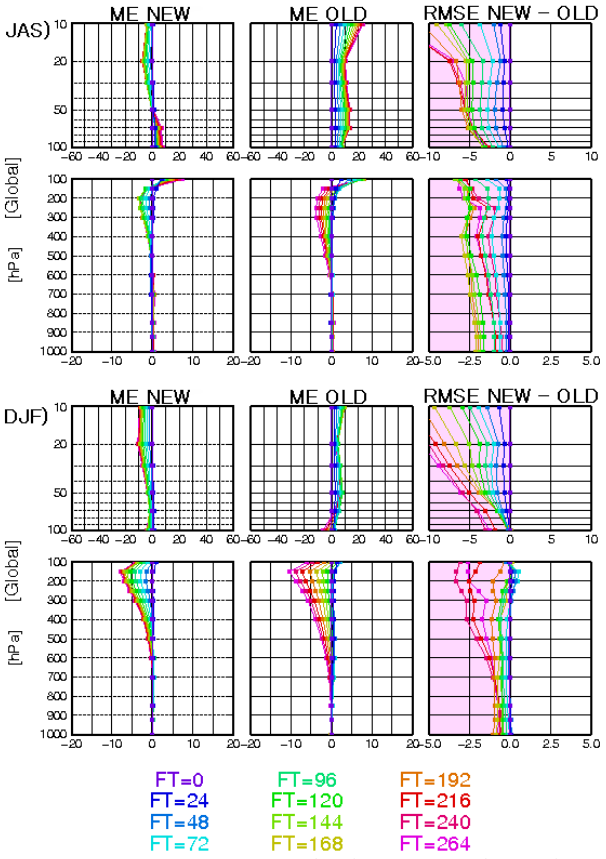

Fig. 2: Profiles of new MEs (left), old MEs (center) and RMSE differences (new – old, right) for geopotential height [m]. The reference values are the respective analysis results, and the verification region is the whole globe. The trial periods are six months for JAS 2013 (top) and DJF 2012/3 (bottom). Each line shows the result of a forecast time from FT = 0h to FT = 264h at 24-hour intervals.

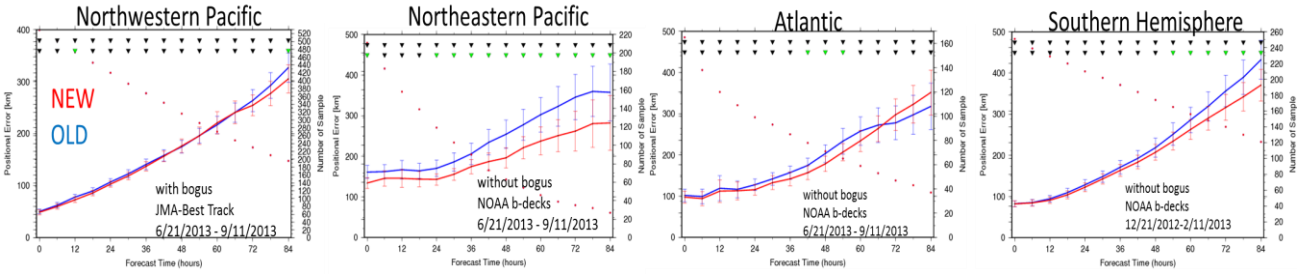

Fig. 3: Tropical cyclone track forecast errors for four regions (Northwestern Pacific, Northeastern Pacific, Atlantic, Southern Hemisphere). References are JMA best track and NOAA b-deck data. Red and blue lines show the track errors of the new and old models respectively (left axis), and each point shows the number of samples (right axis). Error bars indicate the two-sided 95% confidence interval.